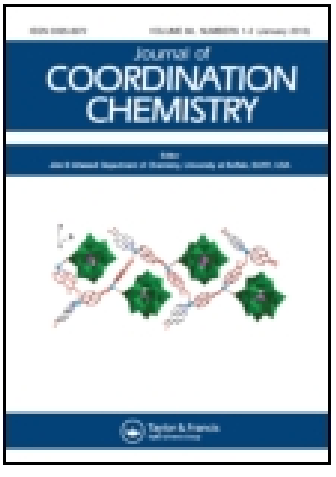

Journal of Coordination Chemistry
Publication details, including instructions for authors and subscription information:
http://www.tandfonline.com/loi/gcoo20

Different coordination patterns for two related unsymmetrical compartmental ligands: crystal structures and IR analysis of $[Cu(C_{21}H_{21}O_2N_3)(OH_2)(ClO_4)]ClO_4{\cdot}2H_2O$ and $[Zn_2(C_{22}H_{21}O_3N_2)(C_{22}H_{20}O_3N_2)]ClO_4$

Aline Cruz De Moraes Reis[a], Maria Clara Ramalho Freitas[b], Jackson A.L.C. Resende[b], Renata Diniz[c] & Nicolás A. Rey[a]

[a] Laboratório de Síntese Orgânica e Química de Coordenação Aplicada a Sistemas Biológicos (LABSO-BIO), Department of Chemistry, Pontifical Catholic University of Rio de Janeiro, Rio de Janeiro, Brazil

[b] Institute of Chemistry, Federal University Fluminense, Niterói, Brazil

[c] Department of Chemistry, ICE, Federal University of Juiz de Fora, Juiz de Fora, Brazil

Accepted author version posted online: 28 Aug 2014.Published online: 18 Sep 2014.

To cite this article: Aline Cruz De Moraes Reis, Maria Clara Ramalho Freitas, Jackson A.L.C. Resende, Renata Diniz & Nicolás A. Rey (2014) Different coordination patterns for two related unsymmetrical compartmental ligands: crystal structures and IR analysis of $[Cu(C_{21}H_{21}O_2N_3)(OH_2)(ClO_4)]ClO_4{\cdot}2H_2O$ and $[Zn_2(C_{22}H_{21}O_3N_2)(C_{22}H_{20}O_3N_2)]ClO_4$, Journal of Coordination Chemistry, 67:18, 3067-3083, DOI: 10.1080/00958972.2014.958080

To link to this article: http://dx.doi.org/10.1080/00958972.2014.958080

Journal of Coordination Chemistry, 2014
Vol. 67, No. 18, 3067–3083, http://dx.doi.org/10.1080/00958972.2014.958080

Different coordination patterns for two related unsymmetrical compartmental ligands: crystal structures and IR analysis of $[Cu(C_{21}H_{21}O_2N_3)(OH_2)(ClO_4)]ClO_4{\cdot}2H_2O$ and $[Zn_2(C_{22}H_{21}O_3N_2)(C_{22}H_{20}O_3N_2)]ClO_4$

ALINE CRUZ DE MORAES REIS†, MARIA CLARA RAMALHO FREITAS‡, JACKSON A.L.C. RESENDE‡, RENATA DINIZ§ and NICOLÁS A. REY*†

†Laboratório de Síntese Orgânica e Química de Coordenação Aplicada a Sistemas Biológicos (LABSO-BIO), Department of Chemistry, Pontifical Catholic University of Rio de Janeiro, Rio de Janeiro, Brazil
‡Institute of Chemistry, Federal University Fluminense, Niterói, Brazil
§Department of Chemistry, ICE, Federal University of Juiz de Fora, Juiz de Fora, Brazil

(*Received 8 November 2013; accepted 10 July 2014*)

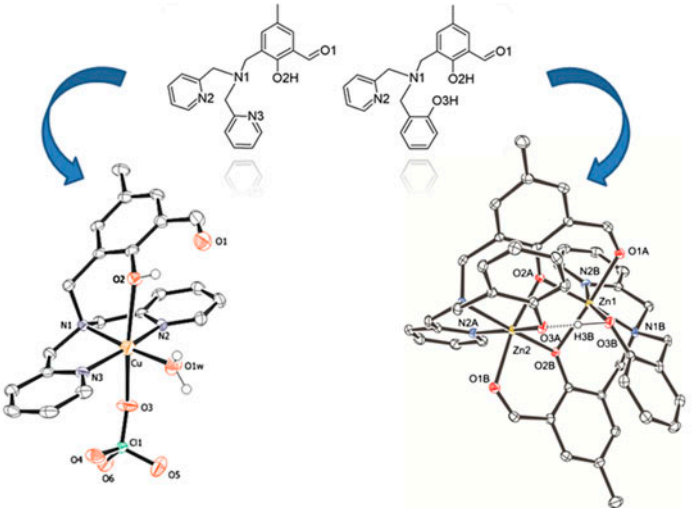

The crystal structures of the new complexes $[Cu(HL1)(OH_2)(ClO_4)]ClO_4{\cdot}2H_2O$ (**1**) and $[Zn_2(HL2)(L2)]ClO_4$ (**2**), derived from two related, phenol-based compartmental ligands, are described. Compound **2** constitutes the first report of a complex obtained from $\mathbf{H_2}\boldsymbol{L2}$. The metal compounds are structurally different; **2** is a dimer in which all the heteroatoms of the ligand take part in coordination, while **1** is mononuclear containing a pair of *cis*-oriented ligands that complete an "open" coordination sphere, in which the aldehyde group of $\mathbf{H}\boldsymbol{L1}$ is not involved. The protonation status of the central phenol groups of $\mathbf{H}\boldsymbol{L1}$ and $\mathbf{H_2}\boldsymbol{L2}$ are also dissimilar between the complexes. Infrared vibrational analyses of both complexes, as well as their respective ligands, were performed to connect the

*Corresponding author. Email: nicoarey@puc-rio.br

observed spectral features with the structural properties of the solids. While some distinctive bands shifted upon complexation, it was not possible to confirm involvement of the aromatic aldehyde group in coordination by this technique. ^{1}H NMR experiments involving **2** suggest that its particular protonation status is maintained upon dissolution in d_6-DMSO.

Keywords: Compartmental ligands; Copper complex; Zinc complex; XRD; IR spectroscopy

1. Introduction

The study of model dinuclear metal complexes has become an important tool for gaining insight into the function of biologically occurring bimetallic cores. Ligands termed compartmental are defined as the class of polydentate, chelating ligands able to bind simultaneously to two metal ions in the presence of two adjacent coordination sites [1]. The recent recognition of the asymmetric nature of a number of polymetallic biosites has greatly increased the interest in unsymmetrical bioinspired ligands [2, 3]. Furthermore, polynuclear complexes derived from such ligands can display catalytic activities [4, 5]. Thus, the design of binucleating ligands capable of generating asymmetric dinuclear complexes is of interest. The compartmental ligands presently studied are **H*L1***, 3-{[bis(pyridin-2-ylmethyl)amino]-methyl}-2-hydroxy-5-methylbenzaldehyde, and the associated compound **H_2*L2***, 2-hydroxy-3-{[(2-hydroxybenzyl)(pyridin-2-ylmethyl)amino]-methyl}-5-methylbenzaldehyde (chart 1), which are classified as phenol-based compartmental ligands, since the donor that acts as an endogenous bridge between the metal centers in the dinuclear complexes is a phenolic oxygen. Moreover, these ligands have different coordination possibilities, and the phenol group (s) can either remain protonated or be deprotonated in their metal complexes. Both **H*L1*** and **H_2*L2*** contain a central *para*-cresol ring, with a tridentate coordinating side arm and an aldehyde carbonyl occupying *ortho*-positions relative to the hydroxyl substituent of this central unit. The coordinating side arm is constituted by a tertiary aminomethyl nitrogen with a pair of 2-methylpyridine substituents (**H*L1***), or by a tertiary aminomethyl nitrogen exhibiting a 2-methylpyridine and a 2-methylphenol as substituents (**H_2*L2***).

The literature reports some complexes derived from these compartmental ligands. de Oliveira *et al.* [6], for example, reported the X-ray structure of two related mononuclear copper(II) complexes containing **H*L1*** and ***L1*$^{-}$**, that, in aqueous solutions, are able to hydrolyze the peptide bonds of bovine serum albumin. Compounds involving other transition metals have also been synthesized, such as the dinuclear cobalt(II) and manganese(II) complexes

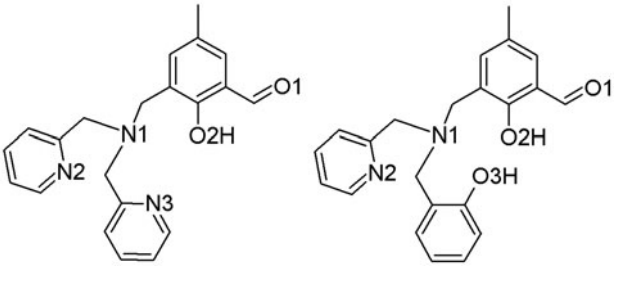

Chart 1. Left: **H*L1*** (3-[*N*,*N*-bis(2-pyridylmethyl)aminomethyl]-5-methylsalicylaldehyde) and right: **H_2*L2*** (3-[*N*,*N*-(2-pyridylmethyl)(2-hydroxybenzyl)aminomethyl]-5-methylsalicylaldehyde).

$[Co_2(L1)_2]^{2+}$ and $[Mn_2(L1)_2]^{2+}$ [7] and a mononuclear dioxovanadium(V) complex, $[VO_2(L1)]$ [8]. Regarding $\mathbf{H_2}\boldsymbol{L2}$, to the best of our knowledge, there are no reports in literature concerning the synthesis of complexes from this ligand. However, this compound was used as a precursor in some studies published by Prof. Ademir Neves' group, at the Federal University of Santa Catarina, Brazil, aimed at preparing higher complexity binucleating ligands [9, 10].

In the present study, the synthesis, crystal structures, and IR vibrational spectra of a new mononuclear copper(II) and a dinuclear zinc(II) complex derived from the phenol-based compartmental ligands $\mathbf{H}\boldsymbol{L1}$ and $\mathbf{H_2}\boldsymbol{L2}$, respectively, are reported.

2. Experimental

2.1. *Materials and methods*

Starting materials were commercially available and were used as purchased. Ligands $\mathbf{H}\boldsymbol{L1}$ [10] and $\mathbf{H_2}\boldsymbol{L2}$ [11] were prepared according to experimental procedures described previously. EA analyses were performed with a Thermo CHNS-O Analyzer Flash EA 1112 Series. Infrared spectra of the compounds were recorded on a Perkin Elmer FT-IR 2000 apparatus. Samples were measured from 4000 to 450 cm^{-1} as KBr pellets.

2.2. *Synthesis*

2.2.1. Preparation of $[Cu(H\boldsymbol{L1})(OH_2)(ClO_4)]ClO_4\cdot 2H_2O$ (1). This complex was obtained by adding a methanolic solution of $Cu(ClO_4)_2\cdot 6H_2O$ (0.5 mM, 0.18 g) dropwise to $\mathbf{H}\boldsymbol{L1}$ (0.5 mM, 0.17 g), dissolved in methanol. The addition of the copper salt immediately resulted in a clear, intense blue color, with no signs of precipitation. The mixture was stirred continuously at 50 °C for 20 min and then left to stand at room temperature for slow evaporation of the solvent. One week later, greenish-blue crystals (0.15 g, 45% yield) suitable for X-ray diffraction (XRD) were observed in the beaker. These were filtered off, washed with cold methanol and diethyl ether, and dried at room temperature (*ca.* 23 °C). Elem. Anal. Calcd for $CuC_{21}H_{27}O_{13}N_3Cl_2$ (%): C, 37.99; H, 4.11; N, 6.33. Found (%): C, 38.38; H, 4.36; N, 6.60.

2.2.2. Preparation of $[Zn_2(H\boldsymbol{L2})(\boldsymbol{L2})]ClO_4$ (2). This complex was synthesized by mixing a methanolic solution of $\mathbf{H_2}\boldsymbol{L2}$ (0.5 mM, 0.18 g) with an excess of $Zn(ClO_4)_2\cdot 6H_2O$ (1.0 mM, 0.37 g). The reaction was stirred at 50 °C for 20 min. A yellow powder was then observed in the reaction flask, which was filtered, washed with cold methanol, dried, and analyzed. However, it was shown to be a by-product and was discarded. The mother liquor was allowed to evaporate at room temperature. After one week, yellow crystals (0.08 g, 34% yield) suitable for X-ray structure determination were obtained. Elem. Anal. Calcd for $Zn_2C_{44}H_{41}O_{10}N_4Cl$ (%): C, 55.51; H, 4.35; N, 5.89. Found (%): C, 55.17; H, 4.54; N, 5.72.

Caution! *Perchlorate salts of metal complexes containing organic ligands are potentially explosive. Only small amounts of material should be prepared, and they should be handled with care.*

Table 1. Crystal, data collection, and refinement parameters for **1** and **2**.

Complex	**1**	**2**
Formula	$CuC_{21}H_{27}O_{13}N_3Cl_2$	$Zn_2C_{44}H_{41}O_{10}N_4Cl$
Formula weight (g M^{-1})	663.90	952.00
Crystal system	Monoclinic	Monoclinic
Space group	$P2_1/n$	$P2_1/c$
a (Å)	8.2905(2)	15.4163(6)
b (Å)	21.5077(4)	11.2120(6)
c (Å)	14.7502(3)	23.5715(1)
β (°)	90.693(2)	93.975(5)
V (Å^3)	2629.9(1)	4064.5(4)
Z	4	4
D_{Calcd} (g cm^{-3})	1.677	1.556
μ (mm^{-1})	3.70	1.312
Refl. measured/unique	14,617/4153	30,160/7456
Observed refl. [$I_{obs} > 2\sigma(I_{obs})$]	3477	6048
No. of refined parameters	361	566
$R(F_o^2/F_o^2 > 2\sigma F_o^2)$	0.0534/0.0428	0.0529/0.037
$wR(F_o^2)$	0.123	0.114
S	1.03	1.12
RMS_{peak} (e$^-$ Å^{-3})	0.080	0.143

2.3. *XRD and powder XRD*

Single-crystal XRD data were collected on an Oxford GEMINI A-ultra diffractometer. For **1**, the measurements were made at 120 K using Cu-K_α (λ = 1.5418 Å) radiation, whereas for **2**, data were obtained at 150 K with Mo-K_α (λ = 0.71073 Å) radiation. Data collection, data reduction, and cell refinement were performed with CrysAlis RED (Oxford Diffraction Ltd, version 1.171.32.38) [12]. Structures were solved and refined using SHELXL-97 [13]. A multiscan absorption correction was applied [14]. All the non-hydrogen atoms were refined anisotropically. Hydrogens bound to carbon were placed at calculated positions and hydrogens bound to oxygen were located from the Fourier difference maps. The coordinates of the phenolic hydrogen in **2** were refined freely. All hydrogens were refined using a riding model. In **2**, the perchlorate was disordered and could be refined over two sets of positions in a 0.85/0.15 ratio. Crystal, data collection, and refinement parameters for **1** and **2** are presented in table 1. Crystallographic figures were drawn employing the ORTEP-3 for Windows [15] and Mercury [16] programs.

The phase purity of both complexes was confirmed by powder XRD (PXRD). PXRD patterns were collected on a Bruker D8 Advance diffractometer, employing Cu-K_α radiation at room temperature. Each sample was scanned between 5° and 40° in 2θ, with 0.02° as step size. A comparison between the experimental PXRD patterns of the isolated materials and those simulated from the single-crystal data by means of the Mercury 3.1 program are in figure S1 (see online supplemental material at http://dx.doi.org/10.1080/00958972.2014.958080).

2.4. *NMR experiments*

^{1}H (for $\mathbf{H_2}\boldsymbol{L2}$ and **2**) and 2-D COSY (only for $\mathbf{H_2}\boldsymbol{L2}$) NMR spectra were recorded at room temperature on a Varian Mercury 200 spectrometer (4.7 T, 200 MHz) using a 5 mm probe and d_6-DMSO as solvent. In the ^{1}H NMR experiments, 128 ($\mathbf{H_2}\boldsymbol{L2}$) or 512 (**2**) scans were acquired and a 45° pulse was employed. The spectra were referenced to the residual solvent peak (2.50 ppm) [17].

3. Results and discussion

3.1. *Description of the crystal structures*

3.1.1. [Cu(H*L1*)(OH_2)(ClO_4)]ClO_4·$2H_2O$ (1). Blue prismatic crystals of **1** crystallized in the monoclinic space group $P2_1/n$. An ORTEP view of the complex is shown in figure 1. Selected bond distances and angles are given in table 2.

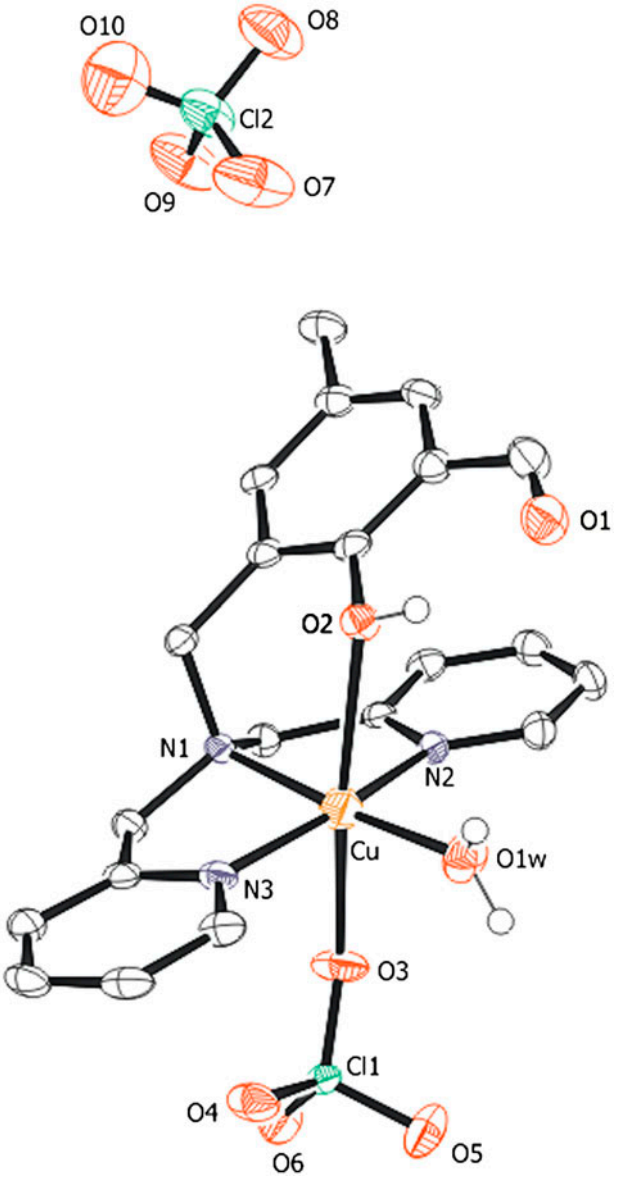

Figure 1. ORTEP of **1** with 50% probability thermal ellipsoids. Hydrogens were omitted for clarity, except for those of the phenol and coordinated water.

Table 2. Selected bond distances and angles for **1**.

Bond	Distance (Å)	Bond	Distance (Å)
Cu–O1w	1.960(3)	Cu–N3	1.983(3)
Cu–N1	2.025(3)	Cu–O3	2.511(3)
Cu–N2	1.977(3)	Cu–O2	2.534(2)
Atoms	**Angles (°)**	**Atoms**	**Angles (°)**
O1w–Cu–N2	94.76(11)	N2–Cu–O2	85.47(10)
O1w–Cu–N3	98.21(12)	N3–Cu–O2	101.22(10)
N2–Cu–N3	165.74(12)	N1–Cu–O2	89.02(9)
O1w–Cu–N1	175.17(12)	O3–Cu–O2	167.89(8)
N2–Cu–N1	84.00(11)	C7–O2–Cu	108.13(19)
N3–Cu–N1	83.55(11)		
O1w–Cu–O3	97.16(11)		
N2–Cu–O3	82.67(10)		
N3–Cu–O3	89.84(10)		
N1–Cu–O3	87.32(11)		
O1w–Cu–O2	86.23(10)		

The crystal structure of **1** reveals a six-coordinate cupric ion in a N_3O_3-distorted environment. **H*L1*** is a tetradentate ligand, coordinating to copper three nitrogens and the central phenol (O2), which remains protonated upon complexation. The nitrogens occupy equatorial positions in the copper coordination sphere, in a plane completed by a coordinated water (O1w). The equatorial copper-donor distances are 2.025(3) Å (Cu–N1), 1.977(3) Å (Cu–N2), 1.983(3) Å (Cu–N3), and 1.960(3) Å (Cu–O1w). O2 occupies one of the Cu axial positions at a distance of 2.534(2) Å. This rather elongated bond, justified by the Jahn–Teller distortion effect, could explain the protonation status of the phenol group. Masuda *et al.* for example, reported a Cu–O distance of 2.601(4) Å for the axially coordinated, protonated, tyrosine phenol in [Cu(Tyr-His)] [18]. Conversely, deprotonated phenol groups display much shorter Cu–O apical coordination distances as, for instance, reported by Rajendran *et al.* [19] for chloro{2-[bis(2-pyridylmethyl)aminomethyl]-4-nitrophenolato} copper(II), 2.268(25) Å. The sixth, and also axial, coordination position in **1** belongs to the perchlorate O3 at a distance of 2.511(3) Å from the metal center. As seen in figure 1, N_3O_3 coordination generates only the *mer*-isomer for the O and N atoms present in the coordination sphere. Among the **H*L1*** heteroatoms, only the aldehyde O1 is not involved in coordination. A second perchlorate, acting as a counter ion, assures the electrical neutrality. In addition, two crystallization water molecules (not shown in figure 1) per $[Cu(HL1)(OH_2)(ClO_4)]^+$ cation were observed.

As pointed out in the introduction, a very similar six-coordinate mononuclear copper(II) complex derived from **H*L1***, $[Cu(HL1)Cl_2]\cdot 2H_2O$, has already been reported [6]. The main difference between this compound and **1** is the presence, in the former, of a pair of coordinated chlorides instead of the water molecule and perchlorate as observed in **1**. As well, Koval and co-workers have prepared the bromide derivative $[Cu(HL1)Br_2]\cdot \frac{1}{2}H_2O$, isostructural to $[Cu(HL1)Cl_2]\cdot 2H_2O$ [20]. Comparison of the bond lengths between **1** and the other copper complexes of **H*L1*** shows that the bond distances in **1** between Cu and the pyridyl N atoms, N2 and N3, are, on average, 0.041 and 0.036 Å shorter than those in $[Cu(HL1)Br_2]\cdot \frac{1}{2}H_2O$ and $[Cu(HL1)Cl_2]\cdot 2H_2O$, respectively. It can also be verified that the N(pyridyl) is a better Lewis base than the tertiary amine (N1), since the Cu–N1 bond distance is longer than the other two distances (table 2). In a previous study, we observed the same behavior

for a zinc(II) complex derived from the mycobactericidal drug isoniazid, with the Zn–N (pyridyl) bond distance shorter than the Zn–N(amine) one [21].

In **1**, the complex ions are packed, leading to a supramolecular structure stabilized by H-bonds and π-stacking interactions, represented in figures 2 and 3, respectively. The H-bond system forms rings that were ranked by degree (size) and complexity: $N_1 = 2R_2^2(8)2R_4^2(10)R_6^6(12)R_6^6(20)$ [22, 23]. All the H-bonds observed in the rings are

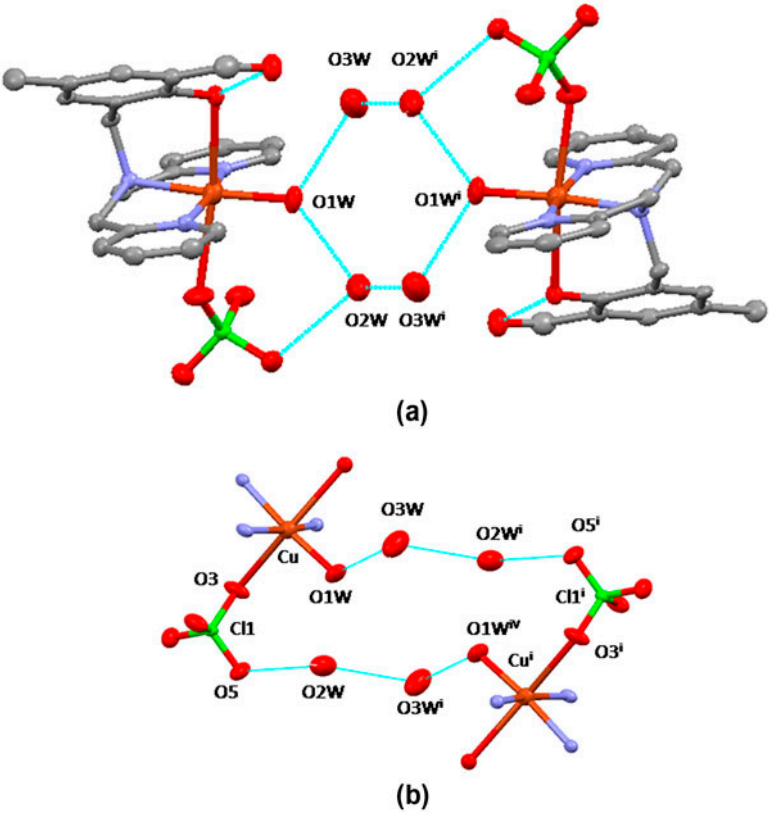

Figure 2. (a) $R_6^6(12)$ ring representation of the H-bonds present in **1**; (b) $R_6^6(20)$ ring formed by the H-bonds. Hydrogens were omitted for clarity; symmetry codes: $i = 2 - x, -y, 2 - z$.

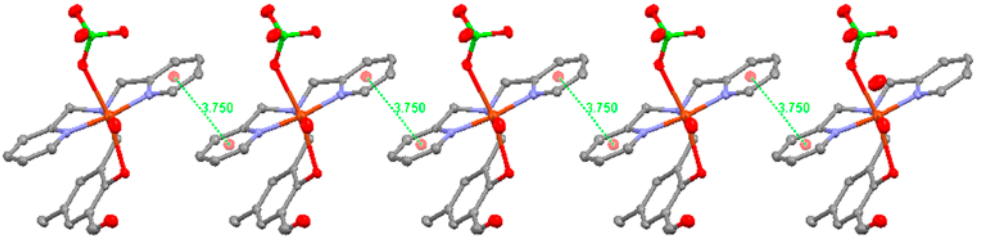

Figure 3. π–π stacking interactions present in **1**.

classified as moderate, i.e. mostly electrostatic, and associated with energies in the range of 4–15 kcal M^{-1}, as can be seen by the donor–acceptor distances in table 3 [24]. An intramolecular H-bond interaction between the O1 (aldehyde) and O2 (phenol) is also present [2.599(4) Å]. The π–π interactions involve both pyridine rings and connect the complex cations, generating linear chains (figure 3). The calculated centroid–centroid distance is equal to 3.750(7) Å.

Table 3. H-bonding parameters for **1**.

Donor-H	*d*(D–H) (Å)	*d*(H···A) (Å)	<DHA (°)	*d*(D···A) (Å)	Acceptor
O2–H2	0.82	1.87	146.7	2.599(4)	O1
O1w–H1w(A)	0.89	1.77	163.9	2.642(4)	O2w
O1w–H1w(B)	0.80	1.86	174.2	2.663(4)	O3w
O2w–H2w(A)	0.85	2.09	144.8	2.827(4)	O5
O2w–H2w(B)	0.86	2.10	146.2	2.857(6)	$O9^{ii}$
O3w–H3w(A)	0.86	2.27	146.7	3.03027(56)	$O8^{ii}$
O3w–H3w(B)	0.89	1.93	176.9	2.820(5)	$O2w^{i}$

Note: Symmetry codes: (i) $-x + 2, -y, -z + 2$; (ii) $x + 1, y, z + 1$.

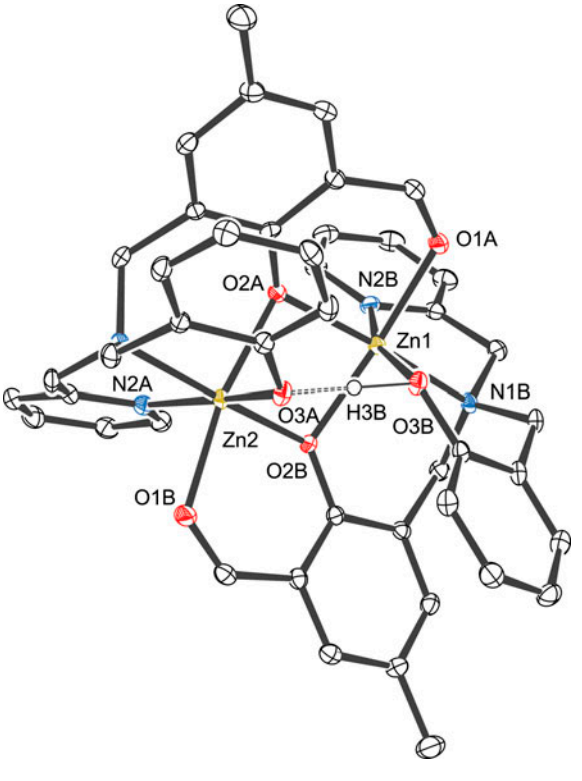

Figure 4. ORTEP of **2** with 50% probability thermal ellipsoids. The perchlorate counterion and all hydrogens, except that of the phenol of the $\mathbf{HL2}^{-}$, were omitted for clarity.

3.1.2. $[Zn_2(HL2)(L2)]ClO_4$, complex 2. Light yellow rectangular crystals of **2** crystallize in the monoclinic system, space group $P2_1/c$. An ORTEP view of **2** is presented in figure 4. Selected bond distances and angles are given in table 4.

The crystal structure of **2** shows a homobimetallic, dimeric cation, with Zn^{2+} cations brought together by deprotonated central phenol groups of two $\mathbf{H_2}\boldsymbol{L2}$-derived ligands, which act as endogenous bridges. Both metal centers are six coordinate, presenting a N_2O_4 coordination sphere. Contrary to **1**, all the potential donors of $\mathbf{H_2}\boldsymbol{L2}$ ligands are involved in complexation. No exogenous or solvent-derived ligands are present.

Each Zn^{2+} cation is coordinated by O3B/O3A (phenol), N1B/N1A (amine), and N2B/N2A (pyridyl) from the side arms of $\mathbf{H}\boldsymbol{L2}^{-}$ B (bound to Zn1) or $\boldsymbol{L2}^{2-}$ ligand A (bound to Zn2). Both tridentate arms act as meridional coordination moieties. The fourth coordination sites are occupied by the aldehyde O1A (Zn1) and O1B (Zn2). The coordination pattern is completed by the two phenoxo bridges mentioned above, O2A and O2B. As a result, distorted octahedral geometries are observed around both Zn^{2+} cations (table 4). The bridging oxygen of one ligand (O2A or O2B) and the aldehyde oxygen of the other (O1B or O1A, respectively) are in a *trans* configuration; O2A–Zn2–O1B is 169.28(8)° and O2B–Zn1–O1A is 165.20(8)°. The Zn1–Zn2 intermetallic distance is 3.0648(5) Å. Compound **2** displays a "butterfly-like" Zn_2O_2 core, with an angle between the two O–Zn–O planes of 21.7°. The O2A–Zn1–O2B and O2B–Zn2–O2A angles are equal to 82.78(8)° and 81.71(8)°, respectively.

Reports on homodinuclear zinc(II) complexes of compartmental ligands are not scarce in literature. Recently, Maiti and co-workers reported dinuclear zinc(II) complexes of (binucleating) phenol-based compartmental ligands displaying coordinating arms derived from

Table 4. Selected bond distances and angles for **2**.

Bond	Distance (Å)	Bond	Distance (Å)
Zn1–O2A	2.038(2)	Zn2–O2B	2.037(2)
Zn1–O2B	2.082(2)	Zn2–O3A	2.092(2)
Zn1–O1A	2.106(2)	Zn2–O1B	2.109(2)
Zn1–N1B	2.107 (3)	Zn2–N1A	2.113(3)
Zn1–N2B	2.125(3)	Zn2–O2A	2.126(2)
Zn1–O3B	2.198(2)	Zn2–N2A	2.132(3)
Zn1···Zn2	3.0648(5)		
Atoms	**Angles (°)**	**Atoms**	**Angles (°)**
O2A–Zn1–O2B	82.78(8)	N2B–Zn1–O3B	164.80(9)
O2A–Zn1–N1B	173.36(9)	O2B–Zn2–O3A	97.81(8)
O2B–Zn1–N1B	93.35(8)	O2B–Zn2–O1B	89.14(8)
O2A–Zn1–O1A	89.12(8)	O3A–Zn2–O1B	88.51(8)
O2B–Zn1–O1A	165.20(8)	O2B–Zn2–N1A	170.50(9)
N1B–Zn1–O1A	95.79(9)	O3A–Zn2–N1A	90.64(9)
O2A–Zn1–N2B	95.92(9)	O1B–Zn2–N1A	95.45(9)
O2B–Zn1–N2B	105.98(9)	O2B–Zn2–O2A	81.71(8)
N1B–Zn1–N2B	79.92(10)	O3A–Zn2–O2A	87.21(8)
O1A–Zn1–N2B	87.11(9)	O1B–Zn2–O2A	169.28(8)
O2A–Zn1–O3B	95.86(8)	N1A–Zn2–O2A	94.42(8)
O2B–Zn1–O3B	85.02(8)	O2B–Zn2–N2A	92.23(9)
N1B–Zn1–O3B	89.14(9)	O3A–Zn2–N2A	169.09(9)
O1A–Zn1–O3B	83.50(8)	O1B–Zn2–N2A	87.38(9)
		N1A–Zn2–N2A	79.71(10)
		O2A–Zn2–N2A	98.51(9)
		Zn2–O2B–Zn1	96.12(8)
		Zn1–O2A–Zn2	94.75(8)

N-ethylpiperidine or *N*-ethylpyrrolidine [25]. The four complexes synthesized by these authors present zinc centers in distorted trigonal bipyramid geometries and intermetallic distances of about 3.27 Å, longer than that observed for **2**. Other examples of homobimetallic, dimeric zinc(II) complexes of phenol-based compartmental ligands have been provided by Asatkar *et al.* [26] and Chakraborty *et al.* [27]. Asatkar and co-workers prepared a series of four unsymmetrical organochalcogen-substituted Schiff bases with a terminal coordinating carbonyl (ketone) group and their respective zinc complexes. One of these complexes had its structure determined by XRD, showing a centrosymmetric molecule containing two equivalent, distorted square pyramidal zinc(II) centers at the distance of 3.232 Å. Terminal chlorides occupy both apical positions and the basal plane is of the NO_3-type. As for **2**, the carbonyl O of one ligand (A or B) in this complex is *trans* to the bridging, phenolate O of the other (B or A, respectively). The Zn–O(carbonyl) distances are 2.097(3) Å, slightly shorter than the values for Zn1–O1A [2.106(2) Å] and Zn2–O1B [2.109(2) Å] in **2**. The work published by Chakraborty and co-workers is especially pertinent because their ligand contains a coordinating pyridine moiety, as in the present study. The authors reported a pair of centrosymmetric dimeric zinc(II) complexes, in which each metal ion is five coordinate and has a distorted trigonal bipyramidal geometry. The Zn···Zn distances [3.2006(5) Å and 3.1969(9) Å] are, once again, greater than that observed for **2**. The Zn–N(pyridyl) bond distances for these complexes [2.1175(17) and 2.124(4) Å] are in agreement with the corresponding Zn1–N2B [2.125(3) Å] and Zn2–N2A [2.132(3) Å] distances in **2**.

Complex **2** exhibits an interesting asymmetry, which is not obvious or even expected considering its dimeric nature. Such a feature is caused by the incomplete deprotonation of $\mathbf{HL2}^{-}$, in which only one phenol group (O2B) loses its proton. Thus, the only difference in the coordination spheres of the metal centers is related to the protonated ($\mathbf{HL2}^{-}$) or deprotonated ($\mathbf{L2}^{\mathbf{2}-}$) states of O3B and O3A from the terminally coordinated phenol groups. As expected, the distances between the Zn centers and these phenolic oxygens are slightly different; the Zn1–O3B distance (2.198(2) Å) is longer than the Zn2–O3A one (2.092(2) Å). Since both ligands in **2** are anionic, one of them completely deprotonated ($\mathbf{L2}^{\mathbf{2}-}$) and the other one partially deprotonated ($\mathbf{HL2}^{-}$), and two Zn^{2+} cations are present in the asymmetric unit (corresponding to the molecular formula), a counter-ion, in this case, a perchlorate anion (not shown in figure 4), is necessary to ensure electrical neutrality. This anion is disordered over two positions. The ligands are not related by symmetry, due to the charge difference between them, which causes a small divergence in some torsion angles. An intramolecular H-bond interaction was observed between O3B–H (phenol) and O3A (phenolate), with a donor–acceptor distance of 2.469(3) Å (table 5), characteristic of a strong, mainly covalent, H-bond [24]. There is no crystallization solvent and neither intermolecular H-bonds nor π-stacking interactions were observed in the structure.

The particular protonation status presented by **2**, involving a terminal phenol coordinated to zinc in its protonated form, has no parallels in the literature concerning dimeric zinc(II) complexes of phenol-based compartmental ligands. Coelho and co-workers [28] reported the structure of the cationic dimer di-μ-chlorido-bis{[2-({[2-(2-pyridyl)-ethyl](2-pyridylmethyl)amino}methyl)-phenol]zinc(II)}, resulting from a tetradentate ligand containing a

Table 5. Intramolecular H-bonding parameters for **2**.

Donor-H	*d*(D–H) (Å)	*d*(H···A) (Å)	<DHA (°)	*d*(D···A) (Å)	Acceptor
O3B–H3B	1.00(4)	1.48(4)	173(3)	2.469(3)	O3A

phenol, two pyridines, and a tertiary amine as coordinating groups. A pair of chlorides is exogenous bridges between the six-coordinate metal centers and both phenolic oxygens remain protonated after complexation. The Zn–O(H) coordination distance is 2.212(3) Å, very close to the value for Zn1–O3B, 2.198(2) Å. Unlike **2**, the dimer described by Coelho *et al. is* centrosymmetric, since both phenol groups are protonated. A. dos Anjos and co-workers published the structure of a mononuclear zinc(II) complex of the hexadentate ligand *N*,*N*′,*N*,*N*′-bis[(2-hydroxy-3,5-di-tert-butylbenzyl)(2-pyridyl-methyl)]-ethylenediamine, in which, as in **2**, one of the ligand's phenol groups remains protonated after complexation [29]. However, contrary to what might be expected, the phenol does not coordinate to the zinc center. Thus, the Zn center in this complex showed a heavily distorted square pyramidal geometry. The coordination distance between the deprotonated phenol group and zinc is 1.904(3) Å, much shorter than that for Zn2–O3A [2.092(2) Å]. This may suggest that, in **2**, the proton H3B is shared to a great degree by O3A and O3B, although it formally belongs to the O3B atom.

There are many structural characteristics that make **2** a curious example of a zinc(II) dimeric complex derived from a phenol-based compartmental ligand. Its asymmetric protonation, involving only one phenol group, prevents the ligands $\boldsymbol{L2}^{2-}$ and $\mathbf{H}\boldsymbol{L2}^{-}$ to be related by symmetry, which results in a non-centrosymmetric species. Six coordination also is not a very common feature in homobimetallic zinc compounds, as well as the presence of a phenol coordinating in its protonated form. Moreover, the inter-metallic distance found in **2** (3.0648(5) Å) is one of the shortest Zn···Zn distances reported to date for compounds of this type. The complexes described by Asatkar *et al.* and Chakraborty *et al.* present centrosymmetric and planar Zn_2O_2 moieties, unlike **2**. For all the literature examples discussed here, the O–Zn–O angles within the four-membered core of each complex are identical, with values of 76.18(12)° (Asatkar [26]) and 78.40(6)° and 78.67(12)° (Chakraborty [27]).

Finally, this work constitutes, to the best of our knowledge, the first description of any $\mathbf{H_2}\boldsymbol{L2}$ complex in the literature.

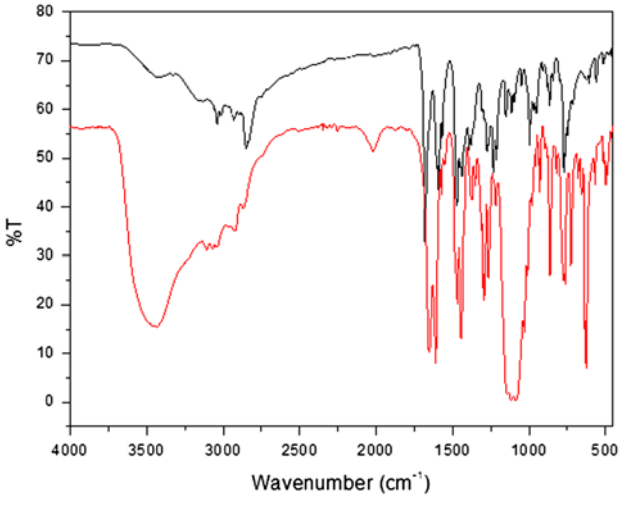

Figure 5. IR spectra of **H*L1*** (black line) and **1** (red line) (see http://dx.doi.org/10.1080/00958972.2014.958080 for color version).

3.2. *IR vibrational spectra analysis*

The infrared spectra of **1** and **2** are very similar, with the main difference related to the perchlorate region (figures 5 and 6, respectively, and table 6). Both complexes show broad bands centered at 3450 cm^{-1}, which are due to the O–H stretches of protonated phenol (**1** and **2**) and the coordinated/crystallization water molecules (**1**). Due to these contributions, the O–H stretching band is stronger in **1**. Other bands related to the phenols are the in-plane δ(C–OH) and ν(C–O) vibrations. In free **H*L1***, the in-plane δ(C–OH) mode provides a single absorption at 1379 cm^{-1}, whereas the **H_2*L2*** spectrum shows two well-defined frequencies, at 1382 and 1352 cm^{-1}, for this vibration. We attribute this to the presence of two non-equivalent phenol groups in **H_2*L2***. Upon complexation, the IR spectra of **1** and **2** show only one band related to this mode, according to their protonation status, which is shifted to lower wavenumber. The ν(C–O) phenol band is also shifted to lower wavenumbers upon coordination, but to a lesser extent (*ca.* 15–20 cm^{-1}).

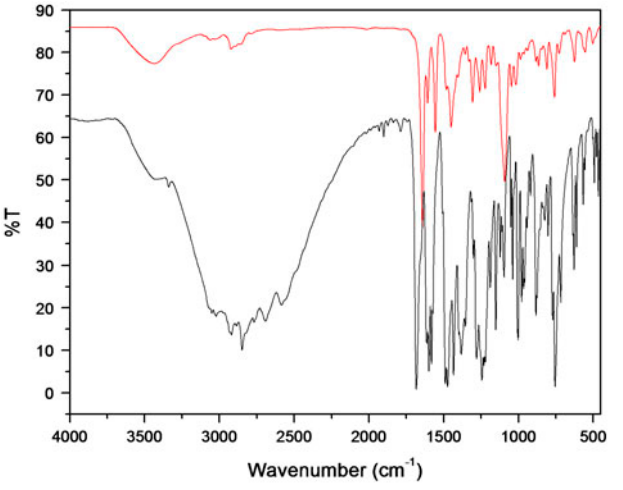

Figure 6. IR spectra of **H_2*L2*** (black line) and **2** (red line) (see http://dx.doi.org/10.1080/00958972.2014.958080 for color version).

Table 6. Selected infrared absorptions, with their respective assignments, for **1** and **2**.

	Infrared vibrational bands (cm^{-1})			
Assignment	**H*L1***	Complex **1**	**H_2*L2***	Complex **2**
ν(C=O)$_{aldehyde}$	1680	1650	1682	1642
Aromatic	1603; 1591	1613; 1574	1600; 1582;	1607; 1556
ν(C=C) and ν(C=N)	1568; 1472	1484; 1468	1475	1480; 1450
Phenol bands:				
δ(C–OH)$_{in\ plane}$	1379	1321	1382; 1352	1306
ν(C–O)	1233	1217	1244	1223
ν(Cl–O)$_{perchlorate}$	–	1116; 1090 (ν_3)	–	1092 (ν_3)
	–	930 (ν_4)	–	939 (ν_4)
		625		

The band associated to the aldehyde ν(C=O) stretch, present at 1680 and 1682 cm^{-1} in the **H*L1*** and **H_2*L2*** spectra, respectively, is shifted to 1650 (**1**) and 1642 (**2**) cm^{-1}. This change is caused by different reasons. In **1**, it is related to the moderate H-bond interaction between this group and the phenol hydrogen. In contrast, in **2**, this slightly more pronounced shift is due to the coordination of the aldehyde to Zn^{2+} cations. The fact that these shifts are very close (30–40 cm^{-1}) leads us to conclude that this ν(C=O) absorption could not be used as a diagnostic band for the inference of the involvement of the aldehyde in coordination. As stated in the introduction, Koval and co-workers prepared dinuclear cobalt (II) and manganese(II) complexes of ***L1***$^-$ [7]. In both compounds, the aldehyde oxygens are coordinated to the metals, and the authors assigned the band present at 1640 cm^{-1} to ν(C=O), with which our proposition agrees. On the other hand, the mononuclear copper(II) complex of **H*L1*** synthesized by de Oliveira *et al.* displays an intense band related to the stretching of its uncoordinated aldehyde group at 1650 cm^{-1} [6]. As in our case, this shift is probably also due to H-bond formation. The dioxovanadium(V) compound of ***L1***$^-$ prepared by Silva *et al.* in which the phenol is uncoordinated and is not involved in intramolecular H bonding, shows its ν(C=O) mode at 1660 cm^{-1} [8]. Concerning the phenol and pyridine aromatic rings, the ν(C=C) and ν(C=N) modes of both **H*L1*** and **H_2*L2*** ligands and **1** and **2** give rise to a series of four bands in the range of 1615–1450 cm^{-1}.

Perchlorate anions display characteristic ν_3 and ν_4 infrared-active modes. As discussed in the crystallographic description of the structures, the number of perchlorate groups present in **1** and **2** is not the same. The perchlorate region of the infrared spectra, as expected, reflects this difference. Complex **2** has a clean pattern, with bands at 1092 (ν_3) and 939 (ν_4) cm^{-1}, typical of a free, uncoordinated tetrahedral ClO_4^- [30]. On the other hand, the ν_3 mode of **1** shows a very complex multi-component envelope, with main frequencies at 1116 and 1090 cm^{-1}, and a series of shoulders. The presence of two ClO_4^- anions and the fact that one of them is coordinated to copper contribute to the splitting of the ν_3 mode. Attempts to relate the energy of the absorptions to the coordination status of ClO_4^- were fruitless. In previous reports published by Rey *et al.* [31, 32], two dinuclear copper(II) complexes containing perchlorate, i.e. $[Cu_2(\mu\text{-OH})(L_{asym})](ClO_4)]ClO_4$ (L_{asym} = 2-[*N*,*N*-di(pyridin-2-ylmethyl)aminomethyl]-4-methyl-6-[(6-methyl-[1, 4]diazepan-6-yl)imino-methyl]phenolate) [31], and $[Cu_2(\mu\text{-OH})(L_{sym})](ClO_4)_2\cdot H_2O$ (L_{sym} = 4-methyl-2,6-bis[(6-methyl-[1, 4]diazepan-6-yl)imino-methyl]phenolate) [32] were synthesized and fully characterized by XRD. Nevertheless, in those studies, the reported infrared bands at 1144, 1110, and 1091 cm^{-1}, and 1147, 1117, and 1082 cm^{-1}, respectively, could not be connected to the structural roles of the ClO_4^- anions. In the IR spectrum of **1**, the ν_4 mode was observed as a single band at 930 cm^{-1}. However, as Lewis and co-workers showed several years ago, the presence of a pair of bands between 700 and 600 cm^{-1}, assigned to the A1 and E modes of a monodentate ClO_4^- anion (C_{3v} symmetry), provides a clear indication of the involvement of this anion in coordination [33]. In the IR spectrum of **1**, an asymmetric band of medium intensity with maximum at 625 cm^{-1} is observed. The ligand **H*L1*** does not show any bands in this region.

3.3. *NMR studies of complex 2 in DMSO solution*

A complete assignment of the hydrogens of free **H_2*L2*** was carried out with a ^{1}H-^{1}H correlation map from a COSY NMR experiment (figure S2, Supplementary material). Figure 7 (bottom) shows the ^{1}H NMR spectrum of **H_2*L2*** in the region ranging from 6.5 to 10.5 ppm, with the respective assignments. The aldehyde (–*H*C=O) hydrogen, as expected,

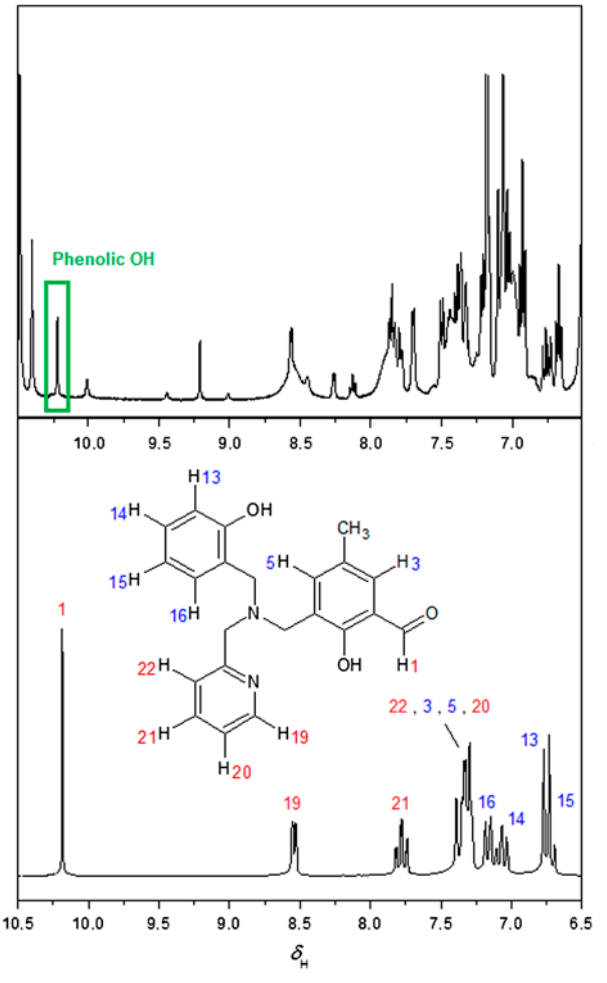

Figure 7. Room temperature ^{1}H NMR spectra (4.7 T, 200 MHz) of $\mathbf{H_2}\boldsymbol{L2}$ (bottom) and **2** (top) from 6.5 to 10.5 ppm. Solvent: d_6-DMSO.

appears as a sharp singlet at the largest ppm value, 10.22 ppm. Among the aromatic hydrogens, those belonging to the pyridine ring are at larger ppm values, especially H19 (8.56 ppm) and H21 (7.79 ppm). Between 7.40 and 7.31 ppm, there is an intricate multiplet corresponding to approximately four hydrogens. This was attributed to the remaining pyridine hydrogens, H22 and H20, and to H3 and H5, the aromatic hydrogens *alpha* to the methyl group. In general, the carbon-bound hydrogens from the phenolic rings are at lower chemical shifts; H16, H14, H13, and H15, which belong to the coordinating side arm, are all observed below 7.20 ppm. The methylene protons could not be seen, since the water band associated with DMSO overlapped. Finally, the methyl hydrogens give a singlet at 2.21 ppm (not shown in figure 7). The ^{1}H NMR spectrum of **2** is also presented in figure 7 (top) for comparison. The presence of the Zn^{2+} cations causes a significant broadening in some of the signals, which could be attributed to the site-exchange processes involving coordination to the metal center [34] and the asymmetry of the $\mathbf{H}\boldsymbol{L2}^{-}$ and $\boldsymbol{L2}^{-}$ ligands.

Because of this, a detailed study on the ^{1}H NMR spectrum of **2** could not be performed. Nevertheless, some differences when compared to the ^{1}H NMR spectrum of the ligand $\mathbf{H_2}\boldsymbol{L2}$ are easily noticeable. The aldehyde hydrogens appear at even larger ppm values upon coordination, at 10.49 ppm. In general, the aromatic protons are at lower ppm values in the spectrum of **2**, but this trend is not valid for all the signals. The presence of a singlet, corresponding to one hydrogen, at 10.19 ppm is assigned to the phenolic hydrogen H3B. This assignment was confirmed by the addition of some D_2O drops to the sample. As expected, the signal disappeared indicating H/D isotopic exchange.

Not many studies involving zinc(II) complexes with ligands containing protonated phenol groups are available in the literature, and even less so with regard to ^{1}H NMR spectroscopy experiments. Among these, to the best of our knowledge, there are no examples in which the protonated phenol group is involved in coordination. Thus, there is no literature value available for comparison of the chemical shifts. Seena and Prathapachandra Kurup [35] studied a series of salicylaldehyde *N*(4)-phenylthiosemicarbazone (H_2L) coordination complexes, in which one of them, $[Zn(HL)_2]\cdot EtOH$, retained a protonated phenol group after complexation. The authors assigned the signal at 11.38 ppm (in $CDCl_3$) to this uncoordinated phenolic proton. Khalil and co-workers prepared a zinc complex of a salicylaldehyde thiosemicarbazone with the formula $[Zn(Tsc)(HTsc)]\cdot H_2O$ [36], with protonated and deprotonated phenol groups, although the former group was not coordinated to zinc. The signal at 10.9 ppm (in d_6-DMSO) was attributed to the phenolic hydrogen.

4. Conclusion

Although similar experimental conditions were employed in the synthesis of **1** and **2**, the resulting metal compounds are quite different. While both the copper and zinc sites are octahedral, **2** is a dimer in which all the heteroatoms of the ligand take part in coordination. On the other hand, **1** is a mononuclear complex in which the aldehyde group of $\mathbf{H}\boldsymbol{L1}$ is not involved in coordination, containing a pair of *cis*-oriented (solvent-derived and perchlorate) ligands that complete an "open" coordination sphere. The protonation status of the central phenol group of $\mathbf{H}\boldsymbol{L1}$ and $\mathbf{H_2}\boldsymbol{L2}$ is also dissimilar between the complexes. Where this group is protonated in **1**, both $\mathbf{H_2}\boldsymbol{L2}$ molecules lose their *para*-cresol phenol protons during the reaction to form **2**. The only phenol proton remaining in **2** belongs to the side arm of one of the $\mathbf{H_2}\boldsymbol{L2}$-derived ligands, and this proton is shared between the two terminally coordinated phenol oxygens. ^{1}H NMR experiments indicated that this particular protonation status is maintained upon dissolution in d_6-DMSO. While IR spectroscopy showed some distinctive band shifts upon complexation, the technique did not exhibit good performance for determining whether the aldehyde carbonyl is coordinated. There are many structural characteristics that make **2** a curious example of a homodinuclear, dimeric zinc(II) complex derived from a phenol-based compartmental ligand. Its asymmetric protonation prevents $\mathbf{H}\boldsymbol{L}^-$ and $\boldsymbol{L}^-$ to be related by symmetry, which results in a non-centrosymmetric species. Also, the presence of a phenol coordinating in its protonated form is definitively not a common feature in homobimetallic zinc compounds. Also, the intermetallic distance in **2** is one of the shortest Zn···Zn distances reported to date for compounds of this type. To the best of our knowledge, **2** constitutes the first report of a complex with $\mathbf{H_2}\boldsymbol{L2}$ in the literature.

Supplementary material

Experimental and simulated PXRD patterns for **1** and **2**; ^{1}H-^{1}H COSY NMR spectrum for $\mathbf{H_2}\boldsymbol{L2}$ (figure S2). Crystallographic data for **1** and **2** have been deposited at the Cambridge Crystallographic Data Center as Supplementary Publications CCDC No. 971141 and 971140, respectively. Copies of the data can be obtained free of charge on application to the CCDC (http://www.ccdc.cam.ac.uk/conts/retrieving.html).

Acknowledgements

The authors gratefully acknowledge financial support from FAPERJ and CAPES. We also thank LabCri-UFMG, for the use of the X-ray facilities, and Prof. Maria Isabel Pais da Silva and M.Sc. Rosana Garrido Gomes (Department of Chemistry, PUC-Rio), for NMR facilities. N.A.R. is grateful to CNPq (Conselho Nacional de Desenvolvimento Científico e Tecnológico, Brazil) for the research fellowship awarded.

References

[1] R. Robson. *Inorg. Nucl. Chem. Lett.*, **6**, 125 (1970).
[2] T. Klabunde, C. Eicken, J.C. Sacchettini, B. Krebs. *Nat. Struct. Biol.*, **5**, 1084 (1998).
[3] E.I. Solomon, U.M. Sundaram, T.E. Machonkin. *Chem. Rev.*, **96**, 2563 (1996).
[4] D. Desbouis, I.P. Troitsky, M.J. Belousoff, L. Spiccia, B. Graham. *Coord. Chem. Rev.*, **256**, 897 (2012).
[5] G. Ambrosi, M. Formica, V. Fusi, L. Giorgi, M. Micheloni. *Coord. Chem. Rev.*, **252**, 1121 (2008).
[6] M.C.B. de Oliveira, M. Scarpellini, A. Neves, H. Terenzi, A.J. Bortoluzzi, B. Szpoganics, A. Greatti, A.S. Mangrich, E.M. de Souza, P.M. Fernandez, M.R. Soares. *Inorg. Chem.*, **44**, 921 (2005).
[7] I.A. Koval, M. Huisman, A.F. Stassen, P. Gamez, M. Lutz, A.L. Spek, D. Pursche, B. Krebs, J. Reedijk. *Inorg. Chim. Acta*, **357**, 294 (2004).
[8] N.M.L. Silva, C.B. Pinheiro, E.P. Chacon, J.A.L.C. Resende, J.W.D. Carneiro, T.L. Fernandez, M. Scarpellini, M. Lanznaster. *J. Brazil Chem. Soc.*, **22**, 660 (2011).
[9] R.A. Peralta, A. Neves, A.J. Bortoluzzi, A. Casellato, A. dos Anjos, A. Greatti, F.R. Xavier, B. Szpoganicz. *Inorg. Chem.*, **44**, 7690 (2005).
[10] R. Jovito, A. Neves, A.J. Bortoluzzi, M. Lanznaster, V. Drago, W. Haase. *Inorg. Chem. Commun.*, **8**, 323 (2005).
[11] S. Uozumi, H. Furutachi, M. Ohba, H. Okawa, D.E. Fenton, K. Shindo, S. Murata, D.J. Kitko. *Inorg. Chem.*, **37**, 6281 (1998).
[12] CrysAlisRED, Version 1.171.32.38, Oxford Diffraction Ltd (Release 17-11-2008 CrysAlis171.NET).
[13] G.M. Sheldrick. *Acta Crystallogr., Part A*, **64**, 112 (2008).
[14] R.H. Blessing. *Acta Crystallogr., Part A*, **51**, 33 (1995).
[15] L.J. Farrugia. *J. Appl. Crystallogr.*, **45**, 849 (2012).
[16] C.F. Macrae, P.R. Edgington, P. McCabe, E. Pidcock, G.P. Shields, R. Taylor, M. Towler, J. van De Streek. *J. Appl. Crystallogr.*, **39**, 453 (2006).
[17] H.E. Gottlieb, V. Kotlyar, A. Nudelman. *J. Org. Chem.*, **62**, 7512 (1997).
[18] H. Masuda, A. Odani, O. Yamauchi. *Inorg. Chem.*, **28**, 624 (1989).
[19] U. Rajendran, R. Viswanathan, M. Palaniandavar, M. Lakshminarayanan. *J. Chem. Soc., Dalton Trans.*, 3563 (1992).
[20] I.A. Koval, M. Huisman, A.F. Stassen, P. Gamez, M. Lutz, A.L. Spek, J. Reedijk. *Eur. J. Inorg. Chem.*, 591 (2004).
[21] M.C.R. Freitas, J.M.S. Antonio, R.L. Ziolli, M.I. Yoshida, N.A. Rey, R. Diniz. *Polyhedron*, **30**, 1922 (2011).
[22] M.C. Etter, J.C. Macdonald, J. Bernstein. *Acta Crystallogr., Part B*, **46**, 256 (1990).
[23] M.C. Etter. *Acc. Chem. Res.*, **23**, 120 (1990).
[24] T. Steiner. *Angew. Chem. Int. Ed.*, **41**, 48 (2002).
[25] P. Maiti, A. Khan, T. Chattopadhyay, S. Das, K. Manna, D. Bose, S. Dey, E. Zangrando, D. Das. *J. Coord. Chem.*, **64**, 3817 (2011).
[26] A.K. Asatkar, S. Nair, V.K. Verma, C.S. Verma, T.A. Jain, R. Singh, S.K. Gupta, R.J. Butcher. *J. Coord. Chem.*, **65**, 28 (2011).

[27] P. Chakraborty, A. Guha, S. Das, E. Zangrando, D. Das. *Polyhedron*, **49**, 12 (2013).
[28] S.E. Coelho, G.G. Terra, A.J. Bortoluzzi. *Acta Cryst.*, **E66**, m229 (2010).
[29] A. dos Anjos, A.J. Bortoluzzi, B. Szpoganicz, M.S.B. Caro, G.R. Friedermann, A.S. Mangrich, A. Neves. *Inorg. Chim. Acta*, **358**, 3106 (2005).
[30] K. Nakamoto, *Infrared and Raman Spectra of Inorganic and Coordination Compounds. Part A: Theory and Applications in Inorganic Chemistry*, 5th Edn, Wiley, New York (1997).
[31] N.A. Rey, A. Neves, A.J. Bortoluzzi, W. Haasec, Z. Tomkowicz. *Dalton Trans.*, **41**, 7196 (2012).
[32] N.A. Rey, A. Neves, A.J. Bortoluzzi, C.T. Pich, H. Terenzi. *Inorg. Chem.*, **46**, 348 (2007).
[33] D.L. Lewis, E.D. Estes, D.J. Hodgson. *J. Cryst. Mol. Struct.*, **5**, 67 (1975).
[34] K.W. Wellington, P.T. Kaye, G.M. Watkins. *Arkivoc*, **17**, 248 (2008).
[35] E.B. Seena, M.R. Prathapachandra Kurup. *Spectrochim. Acta, Part A*, **69**, 726 (2008).
[36] S.M.E. Khalil, M. Shebl, F.S. Al-Gohani. *Acta Chim. Slov.*, **57**, 716 (2010).